On the Effect of Deposition Patterns on the Residual Stress, Roughness and Microstructure of AISI 316L Samples Produced by Directed Energy Deposition

On the effect of deposition patterns on the residual stress, roughness and microstructure of AISI 316L samples produced by Directed Energy Deposition

Gabriele Piscopo[1], Alessandro Salmi[1], Eleonora Atzeni[1], Luca Iuliano[1], Mattia Busatto[2], Simona Tusacciu[2], Manuel Lai[2], Sara Biamino[3], Mostafa Toushekhah[3], Abdollah Saboori[3] and Paolo Fino[3]

[1] Department of Management and Production Engineering, Politecnico di Torino, Italy
[2] IRIS S.r.l., Via Papa Giovanni Paolo Secondo 26, 10043 Orbassano (TO), Italy
[3] Department of Applied Science and Technology, Politecnico di Torino, Italy
gabriele.piscopo@polito.it

Abstract. Despite the extensive capabilities of Laser-Powder Directed Energy Deposition (LP-DED), compared to other metal additive manufacturing processes, the use of LP-DED in industry is still limited as a result of the limited knowledge on the relationships between the process parameters and mechanical behaviour. In this work, the quality of AISI 316L samples, produced by means of LP-DED and evaluated in terms of surface roughness, residual stresses and microstructure, is linked to the scanning strategy. The outcomes confirm that the deposition strategy plays a key role in the definition of the final properties of specimens.

Keywords: Laser Powder-Directed Energy Deposition, 316L, Residual Stress, Surface Roughness, Microstructure.

1 Introduction

Metal Additive Manufacturing (AM) processes are currently recognised as the future of manufacturing industries, thanks to their potentialities in terms of design freedom, part functionality and material usage efficiency [1]. Sectors characterised by a huge level of personalisation, high topological complexity and small production volumes, such as the biomedical, aerospace and racing fields, are the ones in which AM processes are used the most [2]. Focusing attention on processes that use lasers as the energy source to melt material, two different categories of processes can be identified: Laser-Powder Bed Fusion (L-PBF) and Directed Energy Deposition (DED).

Producing large metal components is one of the most challenging issues for AM processes [3]. DED processes allow this problem to be overcome and thus make it possible to produce components in a build volume up to one cubic meter [4]. In the Laser Powder Directed Energy Deposition (LP-DED) process, a focused laser beam is used to produce a melt pool on an existing surface, while a nozzle is used to inject metal powder directly into the generated melt pool. Once the laser moves away, the material rapidly solidifies and a raised track is obtained [5]. The particular LP-DED construction

methodology process allows certain unique capabilities, such as the possibility of repairing worn components, of modifying the topology of an existing component and of producing functionally graded materials (FGMs), to be obtained [1,6]. LP-DED processes are currently considered premature for industrial applications [5]. One of the main reasons is that the properties of the built parts are not sufficiently characterised or optimised. For this reason, it is important to relate the part properties to the main process variables, such as the deposition strategy and process parameters. Smugeresky et al. [7] performed an experimental analysis in order to optimise selected process parameters, that is, the powder size, laser power, scan speed and powder feed rate, with respect to the surface roughness and the microstructure of thin AISI 316L walls produced by means of LP-DED. Pratt et al. [8] used the neutron diffraction method to evaluate the effect of the laser power, scan speed and powder feed rate on residual stresses in thin AISI 410 walls produced by means of LP-DED. Dai and Shaw [9] studied the effects of bi-direction and offset-out scanning strategies on the distortion and residual stresses of single nickel layers produced by means of LP-DED.

The effects of the scanning strategy on the surface roughness, residual stresses and microstructure of AISI 316L stainless steel cubes, produced by means of LP-DED, have been investigated in this work.

2 Materials and methods

The deposition of $20 \times 20 \times 20$ mm^3 AISI 316L stainless steel cubes on a $100 \times 100 \times 8$ mm^3 substrate of the same material was performed using a three-axis machine with a coaxial deposition head. The power source was an ytterbium fibre laser with a maximum operating power of 5 kW. The considered process parameters are listed in Table 1. Two different scanning strategies were adopted:

- 0-90°, an orthogonal deposition direction between two adjacent layers;
- 0-67°, the deposition direction is rotated by 67° for each new layer.

Surface roughness was evaluated on the top and the lateral surfaces of each LP-DED cube sample using a RTP80 portable stylus-type surface-roughness tester (SM Metrology Systems S.r.l, Italy). The measurements were taken along a profile length of 10 mm, using a Gaussian filter and a cut-off of 0.8 mm. Fig. 1 illustrates the directions and the measurement positions that were considered in the experimental analysis according to the following rules:

- the roughness was evaluated on the lateral surfaces along the building direction;
- the first measurement direction on the top surfaces, for the cubes fabricated using the 0-90° scanning strategy, was perpendicular to the scanning direction, the second

Table 1. Process parameters used in the experimental procedure.

Laser power, P	Laser speed, v	Focus, h	Powder feeding rate	Carrier gas flow	Overlap in X	Overlap in Z
900 W	15 mm/s	7.5 mm	3.5 rpm	5 l/min	50%	25%

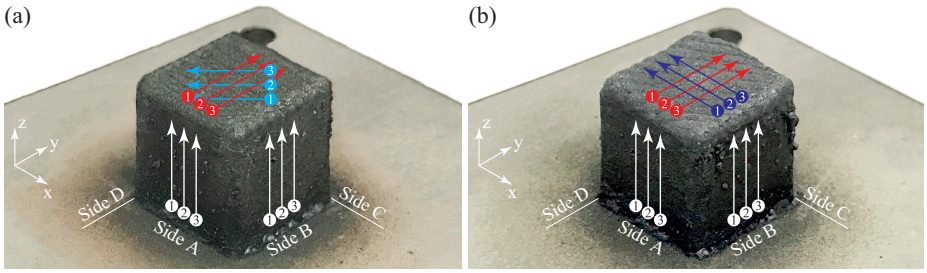

Fig. 1. LP-DED cube samples fabricated using (a) the 0-90° scanning strategy and (b) the 0-67° scanning strategy with lateral surfaces nomenclature and schematic representation of surface roughness measurement directions.

measurement direction was inclined by about −45° with respect to the x-axis, instead the measurement directions for the cubes built using the 0-67° scanning strategy were along the x-axis and along the y-axis.

The residual stress behaviour beneath the surface was evaluated using the semi-destructive hole drilling strain gauge method, according to ASTM E837-13a. The RESTAN-MTS3000 (SINT Technology S.r.l., Italy) system was used. The surfaces of the samples were prepared in order to optimise the bonding between the measuring rosettes and the surface. Thus, agglomerated particles were removed using a flat, high carbon, steel file and the surface was then abraded using abrasive paper with different grain dimensions (120, 400 and 600 grit). The strains released by the tested material were acquired for each drilling step and were used to calculate the residual stresses. An acquisition programme was developed, in LabVIEW 2018, in order to automate the data acquisition at each step. The acquired strains were introduced into EVAL (SINT Technology S.r.l., Italy) software to back-calculate the residual stresses in compliance with the ASTM E837-13a standard. A 1.8 mm diameter drill bit was used in the experimental procedure to produce a 1.2 mm deep flat-bottom hole, by executing 24 drilling steps to a depth of 50 µm. The measurements were performed on the top surface and on Side A (Fig. 1).

3 Results and discussion

The results, in terms of surface roughness, in-depth residual stress profiles and microstructure for the cubes fabricated using the two different scanning strategies, are presented hereafter.

3.1 Surface roughness

From the graph reported in Fig. 2, it is possible to observe that the surface roughness on the lateral surfaces (Side A, Side B, Side C and Side D) is slightly lower than the surface roughness on the top surface. For the cube built using the 0-90° scanning strategy, R_a on the lateral surfaces varies between 20.5 µm and 22.5 µm instead R_a is about 33 µm on the top surface. For the cube built with the 0-67° scanning strategy, the value

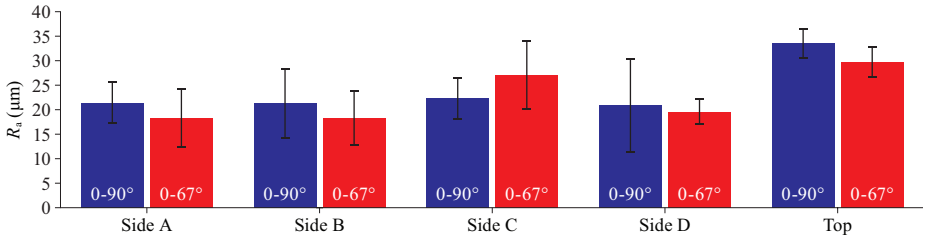

Fig. 2. Surface roughness on the analysed surfaces. The red and the blue bars refer to samples produced using the 0-90° scanning strategy and the 0-67° scanning strategy, respectively.

of R_a on the lateral surfaces varies between 18 µm and 27 µm, whereas the value of R_a is about 29 µm on the top surface.

3.2 Residual stresses

Fig. 3a shows the residual stress distribution on the top surface for both cubes. The oscillatory trend of the residual stresses, with respect to the depth, is clearly noticeable. It is possible to note that the stress distribution is similar for both cubes. The peak of the curves is obtained approximately at the same depth, that is, of 0.7 mm, with a value of about 200 MPa. It may be observed that the direction of the principal stress (β) showed different behaviour when the cubes were fabricated using different scanning strategies. The β-value for the cube produced using the 0-90° scanning strategy is positive for more than half of the analysed depth and then an abrupt variation occurs in correspondence to the maximum stress value. Instead, for the cube produced with the 0-67° scanning strategy, the β-value is prevalently negative, but with an oscillatory trend. Fig. 3b shows the stress distribution on Side A of both cubes. The stresses have

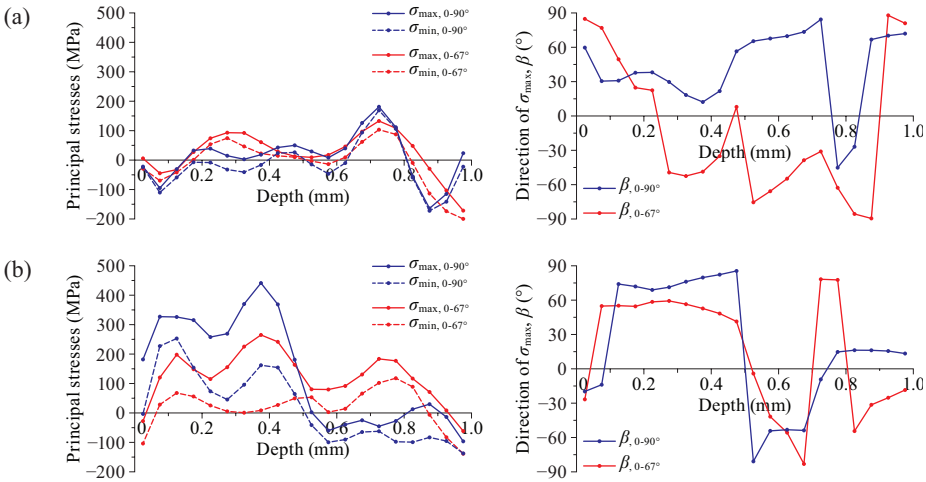

Fig. 3. Stress depth profiles and direction of the principal stress (a) on the top surfaces and (b) on Side A of the cubes.

a similar trend on both cubes. A prevalent tensile stress is observed for a depth of less than 0.5 mm. The maximum stress is obtained at a depth of about 0.4 mm, and it is about 450 MPa in the case of the 0-90° scanning strategy and about 250 MPa with regard to 0-67° scanning strategy. After 0.5 mm, a quite uniform compressive stress, of about 50 MPa, is observed on the cube produced using the 0-90° scanning strategy, instead the stress distribution on the cube produced with the 0-67° scanning strategy shows an oscillatory trend with a predominant tensile state. The trend of the β angle in the two cubes is almost the same. A variation in the β-value occurs at a depth of 0.5 mm. It is possible to relate this behaviour to the value of the residual stress, which crosses the zero-axis and changes in sign from positive to negative.

3.3 Microstructure

In general, the microstructure of each layer of both samples is composed of two regions. The bottom part of each layer is basically a columnar structure. The top part of the layer shows a typical fine cellular dendritic structure with classical secondary dendrite arms that change to a columnar structure in the subsequent deposition. In the laser deposition process, the cooling rate of the melt pool, and consequently the solidification velocity, is very high at the bottom part of the layer. The upper part of the layer cools down slowly compared to the bottom part. Owing to the very high solidification velocity of the bottom part of the melt pool, secondary dendrites were not able to grow. As a result, the bottom part of each layer mainly consisted of primary dendrites. Because of the progressive decrease in the cooling rate from the bottom to the top part of the melt pool, a gradual transition of the microstructure from a fully columnar to a cellular dendritic transition was observed. Fig. 4 shows the microstructure of the cross-section of the cubes deposited with the 0-90° and the 0-67° scanning strategies, respectively. As can be seen in Fig. 4, the Primary Cellular Arm Spacing (PCAS) of the sample produced using the 0-67° scanning strategy is coarser than the cubes produced using the 0-90° scanning strategy. This difference in the PCAS of the cubes produced using different scanning strategies is related to the general cooling rate associated with each rotation.

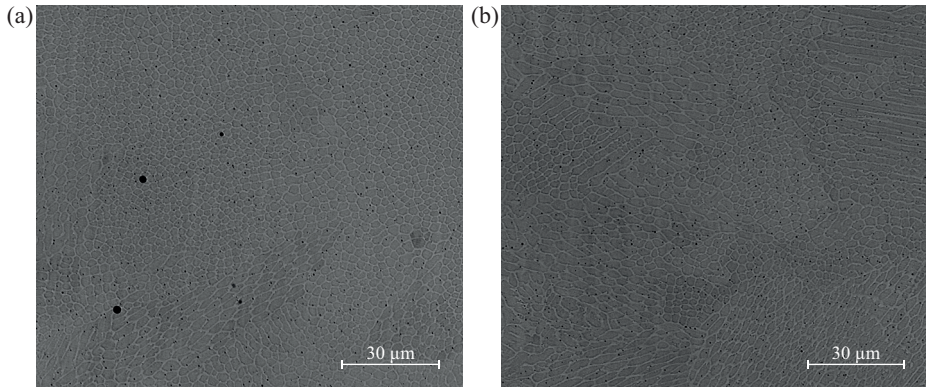

Fig. 4. Microstructure of the cubes obtained using (a) the 0-90° scanning strategy and (b) the 0-67° scanning strategy.

4 Conclusions

In this work, the effect of the adopted scanning strategy on the surface roughness, residual stress and microstructure of cubes produced by means of LP-DED has been investigated. The main results are summarised below:

- the surface roughness on the top surfaces is higher than that on the lateral surfaces. When the 0-90° scanning strategy was used, the surface roughness on the lateral surfaces was about 21 μm and about 33 μm on the top surface, instead when the 0-67° scanning strategy was used, the surface roughness ranged between 18 μm and 27 μm on the lateral surfaces and was about 29 μm on the top surface;
- the residual stresses on the top surfaces were similar for both scanning strategies, although higher stress values were observed on the lateral surfaces of the cubes produced using the 0-90° scanning strategy;
- a coarse microstructure was observed when the 0-67° scanning strategy was used.

Acknowledgments. The authors would like to acknowledge the European Horizon 2020 research and innovation programme; grant agreement No. 723795 / 4D Hybrid–Novel ALL-IN-ONE machines, robots and systems for affordable, worldwide and lifetime distributed 3D hybrid manufacturing and repair operations.

References

1. Gu, D., Meiners, W., Wissenbach, K., Poprawe, R.: Laser additive manufacturing of metallic components: materials, processes and mechanisms. International materials reviews **57**(3), 133-164 (2012).
2. Piscopo, G., Salmi, A., Atzeni, E.: On the quality of unsupported overhangs produced by laser powder bed fusion. International Journal of Manufacturing Research (in press). DOI:10.1504/IJMR.2020.10019045
3. Ngo, T.D., Kashani, A., Imbalzano, G., Nguyen, K.T., Hui, D.: Additive manufacturing (3D printing): A review of materials, methods, applications and challenges. Composites Part B: Engineering **143**, 172-196 (2018).
4. ASTM F3187-16, Standard Guide for Directed Energy Deposition of Metals, ASTM International, West Conshohocken, PA, 2016, www.astm.org. DOI:10.1520/F3187-16
5. Thompson, S.M., Bian, L., Shamsaei, N., Yadollahi, A.: An overview of Direct Laser Deposition for additive manufacturing; Part I: Transport phenomena, modeling and diagnostics. Additive Manufacturing **8**, 36-62 (2015).
6. Toyserkani, E., Khajepour, A., Corbin, S.F.: Laser cladding. CRC press, (2004)
7. Smugeresky, J., Keicher, D., Romero, J., Griffith, M., Harwell, L.: Laser Engineered Net Shaping (LENS [TM]) Process: Optimization of Surface Finish and Microstructural Properties. Advances in Powder Metallurgy and Particulate Materials--1997. **3**, 21 (1997).
8. Pratt, P., Felicelli, S., Wang, L., Hubbard, C.: Residual stress measurement of laser-engineered net shaping AISI 410 thin plates using neutron diffraction. Metallurgical and Materials Transactions A **39**(13), 3155-3163 (2008).
9. Dai, K., Shaw, L.: Distortion minimization of laser-processed components through control of laser scanning patterns. Rapid Prototyping J **8**(5), 270-276 (2002).